

Figure 3.  $\chi_M T$  versus  $T$  plot for 3.

where  $S$  denotes here  $S_{Mn} - S_{Cu} = 2$ .  $J_{intra}$  is directly governed by the nature of the bridge and cannot be modified without changing the copper(II) precursor used in the synthesis. As for  $J_{inter}$ , it might well be related to the interchain separations, since there is no obvious exchange pathway connecting the chains. A careful examination of the structure of **1** (see Figure 1) suggests that this separation along the  $a$  axis is partially controlled by the water molecule in apical position weakly bound to copper ( $Cu-O = 2.417 \text{ \AA}$ ). It follows that if this molecule was selectively removed, the chains might be closer to each other and  $J_{inter}$  increased to some extent.

Warming **1** in the solid phase at  $100 \text{ }^\circ\text{C}$  under vacuum for 48 h affords a new compound of formula<sup>11</sup>  $MnCu(pbaOH)(H_2O)_2$  (**3**). The comparison of the electronic absorption spectra for **1** and **3** in Figure 2 reveals that the water molecule removed belonged to the Cu(II) coordination sphere in **1**. Indeed, the Cu(II) d-d band ( ${}^2B_1 \rightarrow {}^2A_1$  assuming a  $C_{4v}$  symmetry) is shifted from 590 nm in **1** to 555 nm in **3**, as expected when the change is made from a square-pyramidal to a square-planar environment.<sup>12</sup> On the other hand, the energy of the Mn(II) spin-forbidden transition ( ${}^6A_1 \rightarrow {}^4A_1(G) + {}^4E(G)$  assuming an  $O$  symmetry) activated by an exchange mechanism is quasiunchanged (410 nm in **1** and 409 nm in **3**), confirming that the Mn(II) coordination spheres are similar in **1** and **3**.

The  $\chi_M T$  versus  $T$  plot<sup>13</sup> for **3**,  $\chi_M$  being the molar magnetic susceptibility and  $T$  the temperature, shows the minimum characteristic of one-dimensional ferrimagnetic behavior at 120 K (see Figure 3). Actually, **3** behaves magnetically exactly like **1** down to 50 K, indicating that the chain structure is retained and that  $J_{intra}$  keeps the same value ( $-23.4 \text{ cm}^{-1}$ ) in both compounds. On the other hand, when  $T$  is lowered below 50 K,  $\chi_M T$  for **3** increases much more rapidly than for **1**. The ratio  $(\chi_M T)_3/(\chi_M T)_1$  is enhanced from 1 to 3 between 50 and 30 K.<sup>14</sup> This indicates that the spin correlation is much more pronounced in the partially dehydrated compound. This correlation occurs not only along the chain but between the chains as well. The magnetization  $M$  versus  $T$  curves<sup>13</sup> for **3** are shown in Figure 4. The field-cooled magnetization (FCM) measured in cooling down within a field of 5 G shows a rapid increase of  $M$  below ca. 35 K and then a break at 30 K. The zero-field cooled magnetization (ZFCM)

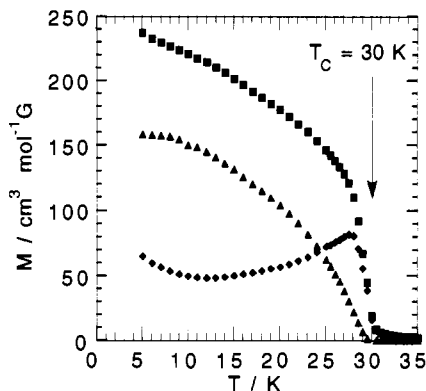


Figure 4. Temperature dependences of the magnetization for  $MnCu(pbaOH)(H_2O)_2$  (**3**): (■) FCM; (◆) ZFCM; (▲) RM.

measured in cooling in zero field down to 5 K and then warming up within the field of 5 G shows a maximum just below 30 K. Finally, the remnant magnetization (RM), obtained in switching off the field at 5 K and warming up in zero field, vanishes at 30 K. These three curves reveal that **3** orders magnetically at  $T_c = 30 \text{ K}$ . At this temperature the slope of the ZFCM versus  $T$  curve is maximum. Below  $T_c$  the variation of  $M$  as a function of the field  $H$  (up to 8 T) is typical of what is expected for a powder magnetic material with a very large zero-field susceptibility and then a rapid saturation.<sup>14</sup> The saturation magnetization is  $M_S = 22.3 \times 10^3 \text{ cm}^3 \text{ G mol}^{-1}$  (or  $4 \mu_B \text{ mol}^{-1}$ ,  $\mu_B$  being the Bohr magneton), which confirms that all the Mn(II) spins are aligned along the same direction and the Cu(II) spins along the opposite direction. The  $M$  versus  $H$  curve<sup>14</sup> presents the same type of hysteresis as what has been reported for **1**, with a coercive field of 60 G at 4.2 K.

Through a mild thermal treatment, we succeeded in shifting  $T_c$  from 4.6 to 30 K, apparently a record in the area of the molecular-based magnetic materials. Since  $J_{intra}$  has not been modified,  $J_{inter}$  may be estimated to have been enhanced by a factor of 40 from eq 1. It is worth mentioning that the same thermal treatment does not give the same effect on **2**. The structural topology of the starting compound plays an essential role.

**Acknowledgment.** We express our deepest gratitude to the Société Nationale Elf Aquitaine, which has financially supported this work and offered a research grant to K.N.

**Supplementary Material Available:** Figures showing the temperature dependence of the ratio  $(\chi_M T)_3/(\chi_M T)_1$  (Figure S5),  $M$  versus  $H$  curve at 4.2 K and up to 8 T (Figure S6), and  $M$  versus  $H$  hysteresis loop at 4.2 K (Figure S7) (4 pages). Ordering information is given on any current masthead page.

Laboratoire de Chimie Inorganique  
URA No. 420  
Université de Paris-Sud  
91405 Orsay, France

Keitaro Nakatani  
Pierre Bergerat  
Epiphane Codjovi  
Corine Mathonière  
Yu Pei  
Olivier Kahn\*

Received March 14, 1991

(10) Richards, P. M. *Phys. Rev. B* 1974, 10, 4687.

(11) Anal. Calcd for  $C_7H_{10}N_2O_9CuMn$  (**3**): C, 21.86; H, 2.62; N, 7.28; Cu, 16.52; Mn, 14.28. Found: C, 21.76; H, 2.51; N, 7.36; Cu, 16.59; Mn, 14.08.

(12) Nakatani, K.; Pei, Y.; Mathonière, C.; Kahn, O. *New J. Chem.* 1990, 14, 861.

(13) The magnetic susceptibility measurements were carried out with a Faraday type magnetometer, and the magnetization measurements with a Métrologie-Ingénierie SQUID magnetometer working in both low-field (a few gauss) and high-field (up to 8 T) modes. The magnetic susceptibility data of Figure 3 were measured within a magnetic field of  $10^3 \text{ G}$ . Those data were corrected for background and core diamagnetism.

(14) Supplementary material.

### The Lithium Chloride Adduct of Monolithiated 5,10-Dihydrophenazine: $[Li_2(\mu-Cl)(\mu-NC_{12}H_8NH)(THF)_4]$

The high polarity of Li–N bonds causes lithium amides to associate,<sup>1</sup> yielding dimers or higher oligomers, depending on the size of the substituents on the N-center and the degree of solvation of lithium.<sup>2–5</sup> Only for exceptionally bulky amides and/or

(1) Setzer, W. N.; Schleyer, P. v. R. *Adv. Organomet. Chem.* 1985, 24, 353.

(2) Engelhardt, L. M.; Jacobsen, G. E.; Junk, P. C.; Raston, C. L.; Skelton, B. W.; White, A. H. *J. Chem. Soc., Dalton Trans.* 1988, 1011 and references therein.

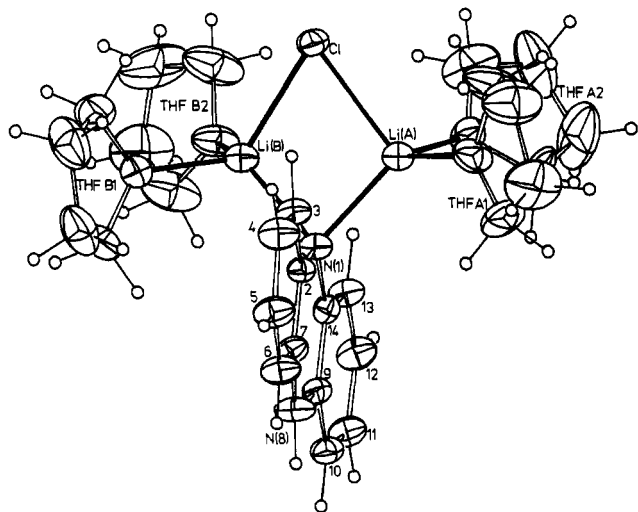
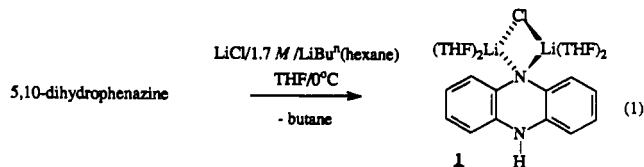


**Figure 1.** Molecular projection of  $[\text{Li}_2(\mu\text{-Cl})(\mu\text{-NC}_{12}\text{H}_8\text{NH})(\text{THF})_4]$  (**1**) with 20% thermal ellipsoids for non-hydrogen atoms and arbitrary radii of 0.1 Å for hydrogen atoms shown. Bond distances (Å) and angles (deg): Cl–Li(A,B) = 2.39 (1), 2.35 (1); N(1)–Li(A,B) = 2.09 (1), 2.06 (1); Li(A)–O(A1,2) = 1.91 (1), 1.97 (1); Li(B)–O(B1,2) = 1.94 (1), 1.97 (1); Li–Li = 2.73 (2); Li(A)–Cl–Li(B) = 70.4 (4); Li(A)–N(1)–Li(B) = 82.4 (5); Cl–Li(A,B)–N(1) = 100.0 (4), 102.4 (5); Cl–Li(A)–O(A1,2) = 113.7 (6), 103.4 (5); Cl–Li(B)–O(B1,2) = 118.3 (6), 104.1 (5); N(1)–Li(A)–O(A1,2) = 116.6 (6), 122.3 (6); N(1)–Li–O(B1,2) = 111.3 (6), 121.8 (6); O( $\pi$ 1)–Li(A,B)–O( $\pi$ 2) = 100.6 (5), 99.9 (6); Li(A)–N(1)–C(2,14) = 109.2 (5), 117.9 (4); Li(B)–N(1)–C(2,14) = 111.7 (5), 116.0 (5).

polydentate ligands are monomeric species formed.<sup>2,3,5,6</sup> Solvated lithium halides can also be monomeric,<sup>7,8</sup> although the tendency is for them to also aggregate.<sup>8–10</sup> Mixed lithium amide/lithium halide aggregates are possible and are of interest because many reactions of lithium amides yield lithium halides, for example in delivering amides to other metal centers.<sup>11</sup> This preformed halide can then associate with unreacted lithium amide, thereby forming complex aggregates. We present the synthesis and first structural characterization of such an aggregate, namely a 1:1 lithium chloride adduct of mono-N-lithiated 5,10-dihydrophenazine. Related to this work is the recent characterization of a complex lithium amide/lithium enolate aggregate; species of this type are implicated in the reactions of lithium amides with enolizable substrates.<sup>12</sup> In addition, the parallel behavior between structures for lithium halides and copper(I) halides is noteworthy<sup>8</sup> and is further highlighted by the formation of copper(I) amide/copper(I) halide aggregates.<sup>13</sup>

Yellow crystals of  $[\text{Li}_2(\mu\text{-Cl})(\mu\text{-NC}_{12}\text{H}_8\text{NH})(\text{THF})_4]$  (**1**) were prepared by treating 5,10-dihydrophenazine and LiCl, in THF, with  $\text{LiBu}^n$  (eq 1).<sup>14</sup> The compound is very air sensitive, de-



composing to the purple phenazhydrin and then finally to phenazine. Decomposition even occurred under “inert conditions”, which hampered microanalyses. Decomposition/oxidation of **1** in  $\text{CCl}_4$  yielded phenazine and THF, in the ratio 1:4 (<sup>1</sup>H NMR), in accordance with the structure established using X-ray diffraction data.

Figure 1 shows the structure of  $[\text{Li}_2(\mu\text{-Cl})(\mu\text{-NC}_{12}\text{H}_8\text{NH})(\text{THF})_4]$  (**1**).<sup>15</sup> Two four-coordinate lithium atoms are bridged by both the chlorine and the anionic N center, thus forming a four-membered Li–N–Li–Cl ring; four-membered rings containing two lithium centers and two amido N or two Cl centers have precedents in lithium amide<sup>2–5</sup> and lithium halide<sup>8</sup> chemistry. The amido ligand is skewed to one side of the  $\text{Li}_2\text{NCl}$  plane (difference in Li–N(1)–C(2) and Li–N(1)–C(14) angles; 8.7 and 4.3° for Li(A) and Li(B), respectively), but the lithium centers are located almost symmetrically on either side of the “phenazine” plane. The Li–Cl distances, 2.39 (1) and 2.35 (1) Å, are similar to those found in the dimeric complex  $[\{\text{Li}(\mu\text{-Cl})(2\text{-methylpyridine})_2\}_2]$ , 2.378 (8) and 2.383 (9) Å,<sup>8</sup> but are shorter than those found in higher lithium chloride aggregates<sup>9,10</sup> and in the complex cation  $[\text{Li}_4\text{Cl}_2(\text{OEt}_2)_{10}]_2^+$ ,<sup>16</sup> where the halides bridge three metal centers. Monomeric species have possibly shorter Li–Cl distances, 2.320 (9) Å in  $[\text{LiCl}(3,5\text{-dimethylpyridine})_3]$ <sup>8</sup> and 2.33 (1) Å in  $[\text{LiCl}(4\text{-tert-butylpyridine})_3]$ .<sup>7</sup> The Li–Cl–Li angle in **1** is rather acute, 70.3 (4)°, compared to those in other aggregates, especially  $[\text{Li}_2(\mu\text{-Cl})(N,N,N',N''\text{-pentamethylethylenediamine})_2]^+$ , which has a linear Li–Cl–Li arrangement and anomalously short Li–Cl distances, 2.17 (3) Å.<sup>17</sup>

The Li–N distances of 2.09 (1) and 2.06 (1) Å are within the limits found for compounds containing four-membered  $\text{Li}_2\text{N}_2$  rings, e.g. 2.082 (6) and 2.296 (7) Å in  $[\{\text{Li}(\mu\text{-N}(\text{Me})\text{Ph}(\text{tmeda}))_2\}_2]$ ,<sup>4</sup> 2.08 (1) and 2.20 (1) Å in  $[\{\text{Li}(\mu\text{-NC}_5\text{H}_4\text{CHSiMe}_3\text{-2})(N,N,N',N'\text{-tetramethylethylenediamine})_2\}_2]$ ,<sup>18</sup> and 1.987 (5) and 2.041 (6) Å in  $[\{2,4,6\text{-Bu}^t_3\text{C}_6\text{H}_2\text{NHLi}(\text{OEt}_2)_2\}_2]$ .<sup>3</sup> The Li–Li distance

- (3) Fjeldberg, T.; Hitchcock, P. B.; Lappert, M. F.; Thorne, A. J. *J. Chem. Soc., Chem. Commun.* **1984**, 823.
- (4) Barr, D.; Clegg, W.; Mulvey, R. E.; Snaith, R.; Wright, S. *J. Chem. Soc., Chem. Commun.* **1987**, 716.
- (5) Lappert, M. F.; Slade, M. J.; Singh, A.; Atwood, J. L.; Rogers, R. D.; Shakir, R. *J. Am. Chem. Soc.* **1983**, *105*, 302. Engelhardt, L. M.; May, A. S.; Raston, C. L.; White, A. H. *J. Chem. Soc., Dalton Trans.* **1983**, 1671. Barr, D.; Clegg, W.; Mulvey, R. E.; Snaith, R. *J. Chem. Soc., Chem. Commun.* **1984**, 285. Haase, M.; Sheldrick, G. M. *Acta Crystallogr., Sect. C* **1986**, *42*, 1008. Armstrong, D. R.; Mulvey, R. E.; Walker, G. T.; Barr, D.; Snaith, R.; Clegg, W.; Reed, D. *J. Chem. Soc., Dalton Trans.* **1988**, 617. Jackman, L. M.; Scarmoutzos, L. M.; Smith, B. D.; Williard, P. G. *J. Am. Chem. Soc.* **1988**, *110*, 6058. Gregory, K.; Bremer, M.; Bauer, W.; Schleyer, P. v. R.; Lorenzen, N. P.; Kopf, J.; Weiss, E. *Organometallics* **1990**, *9*, 1492.
- (6) Power, P. P.; Xiaojie, X. *J. Chem. Soc., Chem. Commun.* **1984**, 358.
- (7) Raston, C. L.; Skelton, B. W.; Whitaker, C. R.; White, A. H. *Aust. J. Chem.* **1988**, *41*, 341.
- (8) Raston, C. L.; Whitaker, C. R.; White, A. H. *J. Chem. Soc., Dalton Trans.* **1988**, 991.
- (9) Raston, C. L.; Skelton, B. W.; Whitaker, C. R.; White, A. H. *J. Chem. Soc., Dalton Trans.* **1988**, 987.
- (10) Barr, D.; Clegg, W.; Mulvey, R. E.; Snaith, R. *J. Chem. Soc., Chem. Commun.* **1984**, 79.
- (11) Lappert, M. F.; Power, P. P.; Sanger, A. R.; Srivastava, R. C. *Metal and Metalloid Amides*; Horwood-Wiley: Chichester, U.K., 1980; p 24.
- (12) Williard, P. G.; Hintze, M. J. *Am. Chem. Soc.* **1990**, *112*, 8602.
- (13) Engelhardt, L. M.; Jacobsen, G. E.; Patalinghug, W. C.; Skelton, B. W.; Raston, C. L.; White, A. H. *J. Chem. Soc., Dalton Trans.*, in press.

- (14) Compound **1** was prepared as follows: A solution of 5,10-dihydrophenazine (0.42 g, 2.30 mmol) and LiCl (0.10 g, 2.30 mmol) in THF (40 mL) was stirred at 0 °C, and  $\text{LiBu}^n$  (1.35 mL, 1.7 M in hexane) was added dropwise. The resulting orange/red solution was stirred at room temperature for 15 min. Reducing the solution to approximately half-volume caused a yellow, microcrystalline precipitate to deposit. The volume of the solution was further reduced to ~15 mL and the red solution filtered from the yellow solid. The precipitate was washed with a cold mixture of THF/hexane (1:1, 25 mL) and dried in vacuo (0.35 g, 29.3%). Microanalysis was hampered by the extreme reactivity of the compound, which was noted by the Canadian Microanalytical Service. Mp: 100–130 °C dec. Infrared:  $\nu_{\text{N-H}}$  3290 (s),  $\nu_{\text{Li-Cl}}$  360 (vs, b), 348 (vs)  $\text{cm}^{-1}$ .
- (15) Crystals of **1** were grown from THF. Crystallographic data ( $T = 296$  K; Syntex P21, diffractometer, crystals mounted in capillaries):  $\text{C}_{22}\text{H}_{21}\text{N}_3\text{O}_4\text{ClLi}_2$ ,  $M_r = 519.0$ , monoclinic, space group  $P2_1/n$ ,  $a = 10.483$  (4) Å,  $b = 16.098$  (7) Å,  $c = 18.453$  (7) Å,  $\beta = 103.53$  (3)°,  $V = 3028$  (2) Å<sup>3</sup>,  $F(000) = 1112$ ,  $Z = 4$ ,  $D_c = 1.14$   $\text{g}\cdot\text{cm}^{-3}$ ,  $\mu$  (monochromatic Mo  $K\alpha$ ) = 1.6  $\text{cm}^{-1}$ , specimen cuboid 0.3 mm (no absorption correction), 2819 unique diffractometer reflections, 1540 with  $I > 3\sigma(I)$  used in the refinement,  $2\theta_{\text{max}} = 40^\circ$ ,  $h,k,\pm l$ . The structure was solved using direct methods and refined by full-matrix least-squares refinement with non-hydrogen thermal parameters anisotropic. Hydrogen atoms were located from difference maps and refined in  $x, y, z, U_{\text{iso}}$ . Residuals at convergence  $R, R'$  were 0.055, 0.047; statistical weights used in the latter were derived from  $\sigma^2(I) = \sigma^2(I_{\text{obs}}) + 0.0005\sigma^4(I_{\text{obs}})$ . Neutral-atom complex scattering factors were used; computation used the XTAL 83 program system implemented on a Perkin-Elmer 3240 computer.
- (16) Hope, H.; Oram, D.; Power, P. P. *J. Am. Chem. Soc.* **1984**, *106*, 1149.
- (17) Buttrus, N. H.; Eaborn, C.; Hitchcock, P. B.; Smith, J. D.; Stamper, J. G.; Sullivan, A. C. *J. Chem. Soc., Chem. Commun.* **1986**, 969.
- (18) Papisergio, R. I.; Raston, C. L.; Skelton, B. W.; Twiss, P.; White, A. H. *J. Chem. Soc., Dalton Trans.* **1990**, 1161.

of 2.73 (2) Å is unexceptional, being similar to that found in dimeric amides<sup>2-5</sup> but significantly shorter than that in dimeric halides, e.g. 3.004 (9) Å in  $[\text{Li}(\mu\text{-Cl})(2\text{-methylpyridine})_2]_2$ ,<sup>8</sup> as expected on the basis of incorporating two third-row atoms into a four-membered-ring system. In general, the bonding in dimeric lithium compounds containing second-row groups is now regarded as highly ionic,<sup>19</sup> and replacing one of the anionic centers by chlorine as in **1** would result in even greater ionic character.

**Acknowledgment.** We gratefully acknowledge support of this work by the Australian Research Council.

**Supplementary Material Available:** Tables listing atomic positional parameters, thermal parameters, ligand hydrogen parameters, extended metal core geometries, and ligand non-hydrogen geometries (10 pages); a listing of structure factor amplitudes (9 pages). Ordering information is given on any current masthead page.

(19) Sannigrahi, A. B.; Kar, T.; Niyogi, B. G.; Hobza, P.; Schleyer, P. v. R. *Chem. Rev.* 1990, 90, 1061.

Department of Chemistry  
University of Western Australia  
Nedlands, WA, Australia 6009

Lutz M. Engelhardt  
Geraldine E. Jacobsen  
Allan H. White

Division of Science and Technology  
Griffith University  
Nathan, Brisbane, Queensland,  
Australia 4111

Colin L. Raston\*

Received June 5, 1991

### Accumulating Evidence for the Selective Reactivity of the 6–6 Ring Fusion of $\text{C}_{60}$ . Preparation and Structure of $(\eta^2\text{-C}_{60})\text{Ir}(\text{CO})\text{Cl}(\text{PPh}_3)_2 \cdot 5\text{C}_6\text{H}_6$

The recent discovery that  $\text{C}_{60}$  (buckminsterfullerene) can be isolated in macroscopic quantities<sup>1,2</sup> has led to widespread interest in its chemical and physical properties.<sup>3</sup>  $\text{C}_{60}$  has icosahedral  $D_{5h}$  symmetry with 20 six-membered rings that are interconnected with 12 five-membered rings. There are two types of C–C bonds within this cluster: one type occurs at the 6–6 ring fusions, while the other occurs at the 6–5 ring fusions. There are no 5–5 ring fusions. Two crystalline derivatives of  $\text{C}_{60}$  have been obtained by addition of transition-metal complexes to the cluster. Addition of osmium tetroxide and *tert*-butylpyridine produces  $\text{C}_{60}\text{O}_2\text{OsO}_2(\text{NC}_3\text{H}_4\text{CMe}_3)_2$  in which an  $\text{O}_2\text{Os}$  unit has added across a 6–6 ring fusion in the carbon cluster.<sup>4</sup> Addition of  $\text{C}_{60}$  to  $(\text{Ph}_3\text{P})_2\text{Pt}(\text{ethylene})$  results in displacement of ethylene and formation of  $(\eta^2\text{-C}_{60})\text{Pt}(\text{PPh}_3)_2$ . In this complex, the platinum atom is bound to carbon atoms again at a 6–6 ring junction of the carbon cluster.<sup>5</sup> Here we report another case of reactivity that involves addition to a C–C bond of a 6–6 ring fusion.

Under a dinitrogen atmosphere, addition of an equimolar amount of a purple solution of  $\text{C}_{60}$ <sup>6</sup> in benzene to a yellow benzene solution of  $\text{Ir}(\text{CO})\text{Cl}(\text{PPh}_3)_2$  immediately forms a deep brown solution from which black-brown crystals of  $(\eta^2\text{-C}_{60})\text{Ir}(\text{CO})\text{Cl}(\text{PPh}_3)_2 \cdot 5\text{C}_6\text{H}_6$  (**1**) precipitate in 45% yield within a matter of minutes. The infrared spectrum of the solid dispersed in a

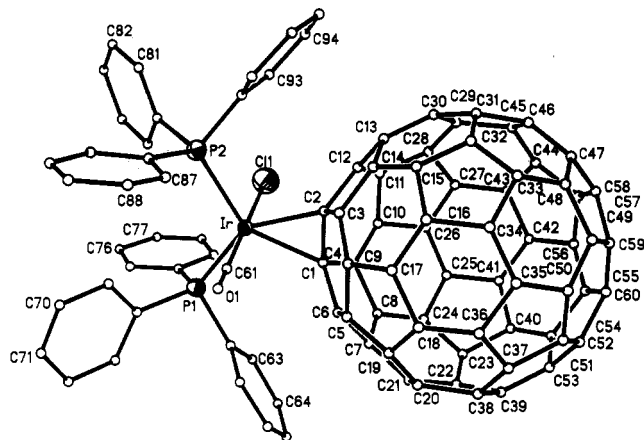


**Figure 1.** Perspective view of  $(\eta^2\text{-C}_{60})\text{Ir}(\text{CO})\text{Cl}(\text{PPh}_3)_2$  with 50% thermal contours for Ir, Cl, and P and uniform, arbitrarily sized circles for C and O. C–C distances within the  $\text{C}_{60}$  range from 1.35 (3) to 1.53 (3) Å. Other bond lengths (Å): Ir–P(1), 2.382 (6); Ir–P(2), 2.385 (7); Ir–Cl, 2.401 (7); Ir–C(1), 2.19 (2); Ir–C(2), 2.19 (2). Bond angles (deg): C(1)–Ir–C(2), 41.0 (8); P(1)–Ir–P(2), 113.3 (2); Cl(1)–Ir–C(61), 179.6 (4).

Fluorolube mull shows  $\nu(\text{CO})$  at 2014  $\text{cm}^{-1}$  (versus 1953  $\text{cm}^{-1}$  for  $\text{Ir}(\text{CO})\text{Cl}(\text{PPh}_3)_2$ ). Crystals suitable for X-ray diffraction have been obtained by slow diffusion of benzene solutions of the reactants into one another.<sup>7</sup> Figure 1 shows a view of the molecule with appropriate atomic labels, while Figure 2 shows a stereoscopic view of the molecule from a different angle. The iridium is attached to the soccer ball shaped  $\text{C}_{60}$  moiety in an  $\eta^2$  fashion through a 6–6 ring fusion. The geometry of the complexed  $\text{C}_{60}$  portion is similar to that observed in the osmium tetroxide<sup>4</sup> and platinum diphosphine<sup>5</sup> adducts. Carbon atoms C(1) and C(2) are pulled away from the  $\text{C}_{60}$  unit toward the iridium. This is best seen by comparing the local structure at C(1) and C(2) with that about C(59) and C(60) at the opposite end of the molecule. The C(1)–C(2) distance of 1.53 (3) Å is at the extreme long end of the range of C–C distances found in **1**. The two triphenylphosphine ligands have folded back into a nearly cis geometry from their trans positions in the starting complex,  $\text{Ir}(\text{CO})\text{Cl}(\text{PPh}_3)_2$ . The carbonyl and chloride ligands retain their trans disposition. The coordination about iridium closely resembles that seen earlier for the tetracyanoethylene (TCNE) complex  $(\text{TCNE})\text{IrBr}(\text{CO})(\text{PPh}_3)_2$  (**2**).<sup>8,9</sup> Thus the Ir–C( $\text{C}_{60}$ ) distances in **1** (2.19 (2) Å) are similar to those in **2** (2.146 (11), 2.151 (11) Å), as are the C–Ir–C angles (41.0 (8)° in **1**; 41.0 (4)° in **2**) and the P–Ir–P angles (113.3 (2)° in **1**; 110.4 (1)° in **2**). The benzene molecules show no unusual contacts with the iridium complex but fill what would otherwise be voids between the molecules (see supplementary material). However, efficient packing within this particular benzene solvate may contribute significantly to the low solubility and isolation of this relatively weakly bound adduct.

Formation of **1** is reversible. Dissolution of the crystalline complex in dichloromethane gives a solution whose infrared spectrum shows  $\nu(\text{CO})$  at 1965  $\text{cm}^{-1}$  due to the presence of  $\text{Ir}(\text{CO})\text{Cl}(\text{PPh}_3)_2$ . No absorption due to **1** is present in the 2100–2000- $\text{cm}^{-1}$  region. The electronic spectrum of this dichloromethane solution is simply a superposition of the spectral features of  $\text{C}_{60}$ <sup>1</sup> and  $\text{Ir}(\text{CO})\text{Cl}(\text{PPh}_3)_2$ . The <sup>31</sup>P NMR spectrum of the complex dissolved in chloroform shows only a resonance at 24.5 ppm, which is the same as that observed for  $\text{Ir}(\text{CO})\text{Cl}(\text{PPh}_3)_2$ .

The formation of **1** adds confirmatory evidence to the suggestion of Fagan and co-workers<sup>5</sup> that  $\text{C}_{60}$ , with its high electron affinity

- Krätschmer, W.; Lamb, L. D.; Fostiropoulos, K.; Huffman, D. R. *Nature* 1990, 347, 354.
- Taylor, R.; Hare, J. P.; Abdul-Sada, A. K.; Kroto, H. W. *J. Chem. Soc., Chem. Commun.* 1990, 1423.
- Reviews: Diederich, F.; Whetten, R. L. *Angew. Chem., Int. Ed. Engl.* 1991, 30, 678. Stoddart, J. F. *Angew. Chem., Int. Ed. Engl.* 1991, 30, 70. Miller, J. S. *Adv. Mater.* 1991, 3, 262.
- Hawkins, J. M.; Meyer, A.; Lewis, T. A.; Loren, S.; Hollander, F. J. *Science* 1991, 252, 312.
- Fagan, P. J.; Calabrese, J. C.; Malone, B. *Science* 1991, 252, 1160.
- $\text{C}_{60}$  was prepared by a modification of the reported arc vaporization of graphite: Haufler, R. E.; Conceicao, J.; Chibante, L. P. F.; Chai, Y.; Byrne, N. E.; Flanagan, S.; Haley, M. M.; O'Brien, S. C.; Pan, C.; Xiao, Z.; Billups, W. E.; Ciufolini, M. A.; Hauge, R. H.; Margrave, J. L.; Wilson, L. J.; Curl, R. F.; Smalley, R. E. *J. Phys. Chem.* 1990, 94, 8634.

- Deep purple plates of  $(\eta^2\text{-C}_{60})\text{Ir}(\text{CO})\text{Cl}(\text{PPh}_3)_2 \cdot 5\text{C}_6\text{H}_6$  crystallize in the monoclinic space group  $P2_1/n$  with  $a = 14.624$  (6) Å,  $b = 19.902$  (12) Å,  $c = 28.388$  (16) Å, and  $\beta = 100.67$  (4)° at 130 K with  $Z = 4$ . Refinement of 4939 reflections with  $F > 4.0\sigma(F)$  and 487 parameters yielded  $R = 0.085$ ,  $R_w = 0.067$ .

- McGinnety, J. A.; Ibers, J. A. *J. Chem. Soc., Chem. Commun.* 1968, 235.

- Manojlović-Muir, L.; Muir, K. W.; Ibers, J. A. *Discuss. Faraday Soc.* 1969, 47, 84.